

## Subthreshold desorption of metastable Ar\* via electron resonances in thin O<sub>2</sub>-doped Ar films

A. D. Bass, E. Vichnevetski, and L. Sanche

*Groupe du CRM en Sciences des Radiations, Faculté de Médecine, Université de Sherbrooke, Sherbrooke, Québec, Canada J1H 5N4*

(Received 14 May 1999)

We report the desorption of metastable argon atoms (Ar\*) stimulated by 11–25 eV electron impact on thin argon films doped with molecular oxygen. The addition of O<sub>2</sub> depletes the metastable atom and photon signals except near 11.5 eV, where it is enhanced due to formation of the  $^2P\text{Ar}^-$ , electron-exciton complex. The enhancement derives from the transfer of an electron from a temporary  $^2P\text{Ar}^-$  ion to an O<sub>2</sub> molecule, forming a stable O<sub>2</sub><sup>-</sup> and an Ar\* that subsequently desorbs at an incident electron energy lower than that of the first exciton of Ar. Time-of-flight measurements indicate that metastable atoms desorbing via the  $^2P\text{Ar}^-$  state have a higher kinetic energy than those desorbed via the direct formation of the  $n=1$  and  $1'$  excitons at higher electron impact energies. A preliminary model for desorption via the anion state is presented.

[S0163-1829(99)07743-7]

### INTRODUCTION

Excitation pathways within rare-gas solids have been<sup>1</sup> and remain an active area of theoretical and experimental investigation<sup>2–4</sup> since this group of materials presents conceptually simple models for dielectric and insulator behaviors. Numerous experimental techniques have been employed to study the electronic structure and the evolution of excitation within these simple materials and in recent years much information has been gained by measurements of photon and electron stimulated luminescence and excited particle desorption from thin rare-gas films.<sup>2</sup>

In general, both the ejection of metastable rare-gas atoms and photon emission can be correlated to the production of free-exciton states within a rare-gas solid.<sup>2</sup> Such excitons propagate freely through a rare-gas solid before trapping at defects or self-trapping as excited atomic or excimer centers. The self-trapping process is rapid but decreases with increasing atomic number.<sup>2,5</sup> For the cases of Ar and Ne, metastable atom desorption may occur when an exciton is trapped as an excited metastable atom close to the film surface. Since both Ar and Ne solids possess a negative electron affinity, the diffuse electronic cloud surrounding a metastable atom interacts repulsively with the surrounding rare-gas medium, a cavity forms, and the metastable is expelled into vacuum.<sup>2</sup> This mechanism for metastable atom desorption, termed ‘‘cavity expulsion’’ (CE), is associated with excitation of the lowest  $n=1$  and  $1'$  surface and bulk excitons and the decay of higher excitons into these states.<sup>2</sup> The kinetic energies (KE) of metastable atoms expelled via CE are typically a few tens of meV.<sup>6–9</sup> Desorbed metastables of higher KE are observed by directly exciting excitons of  $n \geq 2$  and derive from the dissociation of excited ‘‘antibonding’’ excimer states.<sup>2,6,9</sup> The CE of excited rare-gas excimers may also occur and contributes to the luminescence signal along with photons from the decay of short-lived atomic and excimer centers within the film.<sup>2</sup>

In addition to the neutral excitonic structure, electron impact experiments on thin rare-gas films have identified ‘‘electron-exciton complex’’ states which can both couple to dissociative anion states of surface adsorbed molecules<sup>10,11</sup>

and excite phonon mode losses.<sup>12,13</sup> These latter experiments identified the electron-exciton complex as a Feshbach resonance<sup>14</sup> derived from the atomic configuration ( $\dots 3p^5, 4s^2$ )  $^2P_{3/2}$  and  $^2P_{1/2}$ , and formed by the temporary binding of an electron to the lowest bulk excitons. The width of the resonance feature was greater than the spin-orbit splitting for Ar and the state was assigned as  $^2P\text{Ar}^-$  and can be considered the unresolved condensed phase equivalent of the lowest two gas phase Feshbach resonances.<sup>15</sup>

Recent experiments on the electron stimulated desorption (ESD) of metastable Ar atoms<sup>16</sup> (Ar\*) have revealed a resonant contribution to the Ar\* yield, although the  $^2P\text{Ar}^-$  resonance lies several hundred meV below the first bulk exciton state. The resonant contribution arises when the  $^2P\text{Ar}^-$  ‘‘decays’’ into a higher-lying exciton state which subsequently traps and initiates the desorption of an Ar\*. To occur, the process requires that the energy necessary to form the  $n=1$  or higher excitons be released by the transfer of the excess electron from the  $^2P\text{Ar}^-$  into a subvacuum state of the substrate. The resonant contribution is observed only when Ar is adsorbed onto a substrate for which the bottom of the conduction band  $V_0^S$  (measured with respect to the vacuum level) satisfies the following relation:

$$V_0^S \leq -|E_B - V_0| \quad \text{or} \quad V_0^S \leq \Delta E. \quad (1)$$

Here  $V_0$  represents the bottom of the conduction band in the Ar film and  $E_B$  is the binding energy of the resonance relative to  $V_0$ ,  $\Delta E$  is the difference in energy between the resonance and the lowest exciton state. Previously,  $E_B$  was found to be in the range 0.5–0.55 eV,<sup>12,13</sup> while  $V_0$  is 0.3 eV.<sup>17</sup> Thus from Eq. (1) we see that a  $V_0^S \leq -0.2$  or  $-0.25$  eV is necessary for the desorption mechanism to proceed.

The resonant contribution to metastable atom desorption was observed from Ar films of less than 20 monolayer (ML) thickness.<sup>16</sup> The substrate sensitivity of the effect was demonstrated by depositing Ar films onto a Pt substrate and onto Kr, Xe, and  $n$ -hexane films of differing  $V_0^S$ . The involvement of an anionic state was apparent in the variation of the resonance energy as the distance between the Ar film and the supporting Pt substrate was altered by inserting a Xe film of

varying thickness. Similar shifts in resonance energy have been observed in other systems, notably for the  $^2\Pi_u$  resonance of  $N_2$  deposited onto the surface of various rare-gas solids,<sup>18</sup> and are known to derive from the film thickness dependent changes in polarization energy.

Our earlier experiments on the desorption of  $Ar^*$  via formation of the electron-exciton complex<sup>16</sup> suggest that a similar excitation pathway could exist when a rare gas is doped with a molecular impurity capable of trapping a subvacuum energy electron. Such a process might have significant implications for the physics of heterogeneous films and clusters and would be of basic fundamental interest. In this paper, we investigate this topic by studying mixture films of Ar and  $O_2$  deposited onto Pt and onto crystalline  $n$ -hexane substrates. We measure the luminescence and metastable atom yield as a function of incident electron energy and  $O_2$  concentration. The data show that  $O_2$  via formation of the  $^2\Pi_g O_2^-$  anion does indeed provide a suitable electronic trap and thus allows metastable atom desorption via excitation of the  $^2P Ar^-$  state. We also present time-of-flight (TOF) data that show an increased KE for Ar metastable atoms desorbing via the  $Ar^-$  state. Possible reasons for this surprising result are discussed in the text.

## EXPERIMENT

Experiments were performed in an ultrahigh vacuum system, capable of reaching a base pressure of  $\sim 4 \times 10^{-11}$  Torr. The instrument, a detailed description of which has been given elsewhere,<sup>7</sup> consists of an electrostatic electron monochromator, a cryogenically cooled Pt crystalline substrate, hemispherical mesh grids, and a position sensitive detector. Typically, an incident electron beam of 5-nA current and energy resolution of 60 meV [full width at half maximum (FWHM)] is used. The energy of the electron beam is known relative to vacuum level to  $\pm 0.1$  eV.<sup>17</sup> Potentials applied to the mesh grids allow only neutral particles (NP) (i.e., photons and metastable atoms) to be detected. Pulsing the electron beam permits TOF measurements and/or the separation of photon and metastable signals. However, due to low count rates, most of the data presented here represents a combined photon/metastable yield whose variation with incident electron energy is referred to as the NP excitation function.

Target films are grown on the Pt (111) surface by condensing from the vapor phase Ar,  $O_2$ , and  $n$ -hexane. An alternative substrate for the Ar/ $O_2$  experiments was prepared by depositing  $n$ -hexane onto the Pt at 70 K. At this latter temperature, a crystalline surface is formed such that diffusion of Ar and  $O_2$  (deposited at 20 K) into the  $n$ -hexane layer is minimized.<sup>19</sup> The Ar and  $O_2$  gases were supplied by Matheson of Canada Ltd., with stated purities of 99.9995% and 99.995%, respectively. The purity of  $n$ -hexane was better than 99.9%. Film thicknesses are estimated to  $\approx 30\%$  accuracy from the calibrated amount of gas needed to deposit a monolayer, assuming no change of the sticking coefficient for the adlayers, as previously described.<sup>7,20</sup> Heterogeneous Ar/ $O_2$  films are prepared by simultaneous deposition of the gases. The composition of such films is assumed to that given by their partial pressures as measured in a manifold prior to deposition. Molecular oxygen is known to substitute

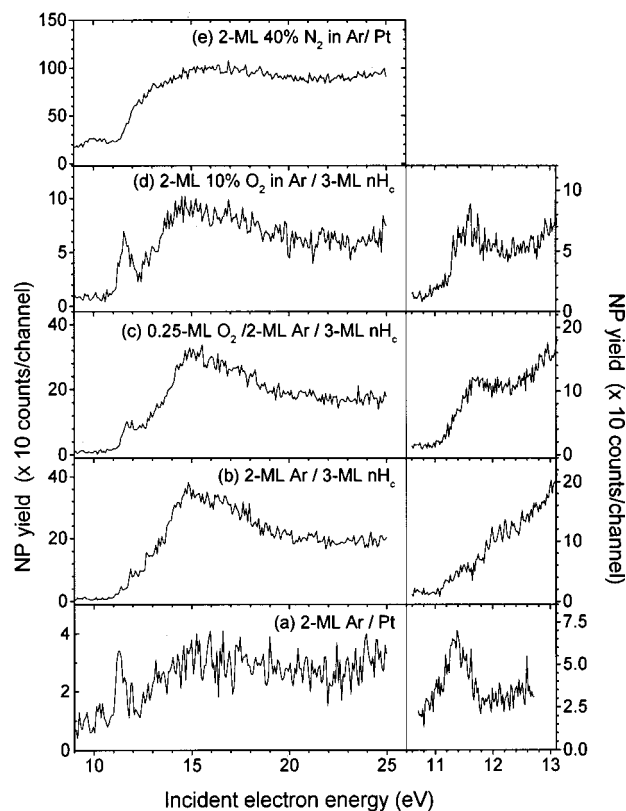


FIG. 1. Neutral particle yields as a function of incident electron energy. (a) 2 ML of Ar deposited onto Pt. (b) 2 ML of Ar deposited on 3 ML of crystalline  $n$ -hexane  $nH_c$  (70 K). (c) 0.25 ML of  $O_2$  deposited onto 2 ML of Ar on 3 ML of  $n$ -hexane. (d) 2 ML of a 90% Ar/ 10%  $O_2$  mixture deposited onto 3 ML of  $nH_c$  (70 K). (e) 2 ML-thick film of a 60% Ar/40%  $N_2$  mixture. Right-hand panels show resonant structure with improved statistics.

readily for Ar in a matrix, such that homogeneously distributed films containing as much as 60%  $O_2$  can be grown.<sup>21</sup>

Films of Ar condensed onto Pt or crystalline  $n$ -hexane are labeled in figures as Ar/Pt or Ar/ $nH_c$ , respectively. A numerical prefix indicates the film thickness, e.g., 2-ML Ar/5-ML  $nH_c$ , for a 2-ML film of Ar deposited on a 5-ML  $n$ -hexane film. The percentage composition of  $O_2$  in Ar/ $O_2$  mixtures is also indicated, for example, spectra from a 3-ML-thick film of a volumetric mixture of 10%  $O_2$  and 90% Ar deposited onto the platinum target would be 3-ML 10%  $O_2$  in Ar/Pt.

## RESULTS

Figure 1 shows the NP excitation functions from several thin films of differing preparation and illustrates the effect of molecular oxygen on condensed Ar. In the lowest panel [Fig. 1(a)] we present the yield from a 2-ML-thick film of pure Ar, where at an energy of  $\sim 11.5$  eV one can observe the narrow feature (FWHM  $< 0.4$  eV) associated with  $Ar^*$  desorption via formation of the  $2P Ar^-$  electron-exciton complex. This resonance peak is shown on an extended energy scale in the right-hand panel of Fig. 1. The signal at higher energies is correlated to production of neutral excitons within the film and their decay by metastable ejection and/or photon luminescence.<sup>6</sup> The maximum NP yield at  $\sim 15$  eV coincides

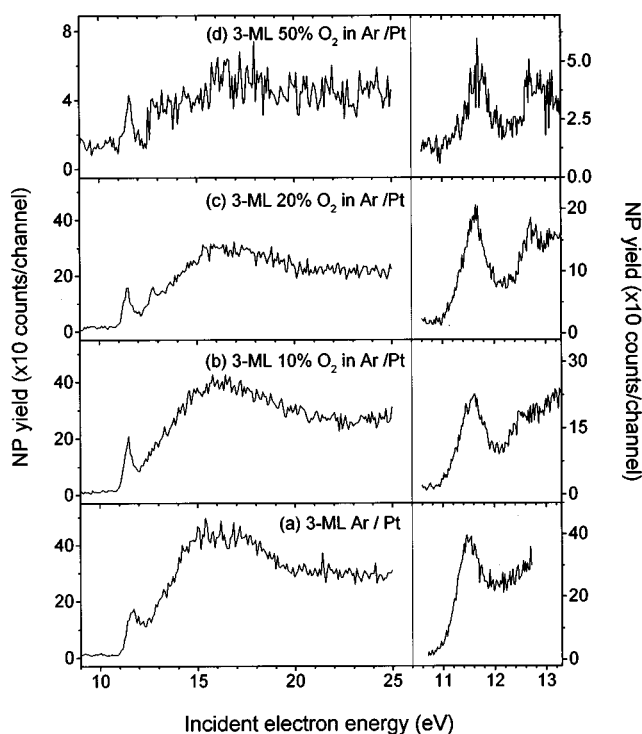


FIG. 2. The effect of increasing  $O_2$  concentration on the NP yield functions from 3-ML-thick Ar/ $O_2$  mixtures. (a) Pure Ar, (b) 10%  $O_2$ , (c) 20%  $O_2$ , (d) 50%  $O_2$ . All films were deposited directly onto the Pt substrate. Right-hand panels show resonant structure with improved statistics.

with the energy for optimum production of excited states in the gas<sup>22</sup> and condensed phases.<sup>6</sup>

Since observation of the  $^2P$  resonance requires that an electron be transferred from the  $Ar^-$  to a subvacuum substrate state,<sup>16</sup> the feature is absent when Ar is deposited onto crystalline *n*-hexane [Fig. 1(b)] for which  $V_0^S$  is +0.8 eV.<sup>23</sup> In contrast,  $Ar^*$  production is enhanced near the resonance energy when a small submonolayer quantity of  $O_2$  is deposited on the surface of the Ar film [Fig. 1(c)]. The resonant nature of this enhancement is more apparent when a 10% concentration of  $O_2$  is incorporated within the Ar matrix, as shown in Fig. 1(d). [It is possible that the small NP signal seen near the resonance in Fig. 1(b), is due to contamination of Ar and/or *n*-hexane in the gas handling system prior to deposition.] We note that no appreciable photon or metastable signal was observed from pure films of molecular  $O_2$  with electrons of less than  $\sim 20$  eV. For comparison, Fig. 1(e) shows the NP excitation function from an  $N_2$ -doped Ar film. Neither the inclusion at 40% concentration within an Ar matrix [Fig. 1(e)] or the addition of  $N_2$  to the surface of an Ar film (not shown) enhances NP production via the  $^2P$   $Ar^-$ . In fact, the resonance is completely absent from the figure while a signal centered near 10 eV and associated with the desorption of  $N_2$  metastables is clearly visible.<sup>24</sup>

An enhancement in NP production via the  $Ar^-$  state relative to other processes, is also evident in Fig. 2, which compares the NP excitation functions from Ar/ $O_2$  matrices of increasing  $O_2$  concentration. The Ar/ $O_2$  films displayed in the figure were formed by deposition directly onto the Pt substrate. Figure 2(a) shows the NP excitation function for

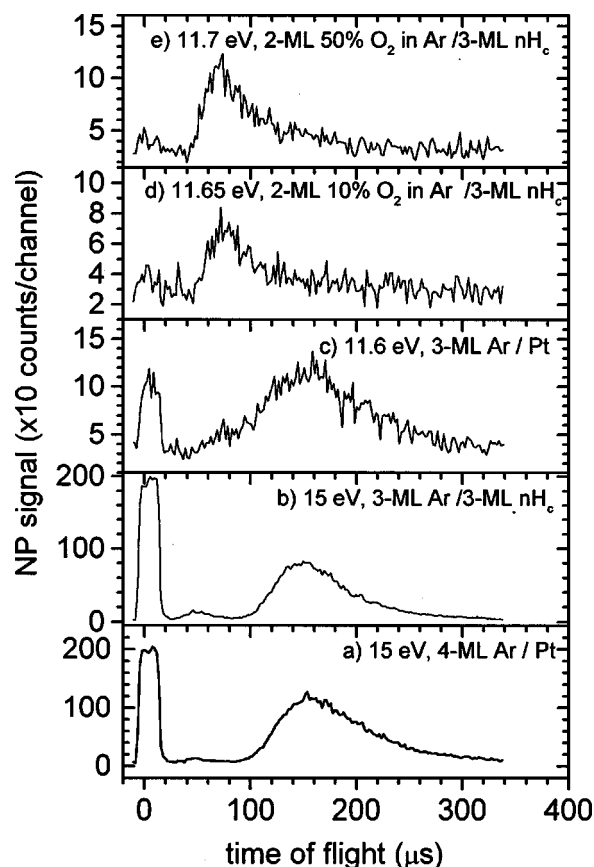


FIG. 3. Time-of-flight spectra of emitted photons and desorbed  $Ar^*$  obtained at the indicated electron impact energies from films of the indicated composition.

3-ML of pure Ar. As in Fig. 1(a), the  $^2P$   $Ar^-$  feature is readily apparent due to electron transfer into the metal. In Fig. 2(b), an enhancement in the intensity of this feature is seen for an Ar matrix containing 10%  $O_2$ . Increasing the  $O_2$  concentration further [Figs. 2(c) and 2(d)] enhances the resonant  $Ar^*$  channel relative to the other direct processes responsible for metastable desorption and photon emission. The feature is also observed to decrease in width and to shift to higher energy as the  $O_2$  concentration is increased.

Time-of-flight (TOF) spectra recorded for films of differing composition, at resonance and at an incident energy of 15 eV, are presented in Fig. 3. For example, Fig. 3(a) shows a TOF spectrum obtained with an incident electron energy of 15 eV from a 3-ML-thick Ar film deposited onto the Pt monocrystal. As in earlier studies, the TOF spectrum is seen to consist of three structures: a photon peak at  $t=0$   $\mu s$  and two slower components at  $\sim 50$   $\mu s$  and  $\sim 150$   $\mu s$ , which are associated with the desorption of metastable atoms via respectively, the dissociation of excimerlike trapped excitons and the CE of atomlike trapped excitons.<sup>2,7</sup> Angular ESD measurements have indicated that the slow metastable signal can be resolved into three subcomponents with distinct KE.<sup>7</sup> This result was consistent with calculations by Cui, Johnson, and Cummings<sup>8</sup> which showed that for desorption from an imperfect surface, the KE of an ejected  $Ar^*$  atom depended on the number of nearest neighbors. Since the present data were collected over a large solid angle using the entire surface of our detector, the data is dominated by the slowest CE

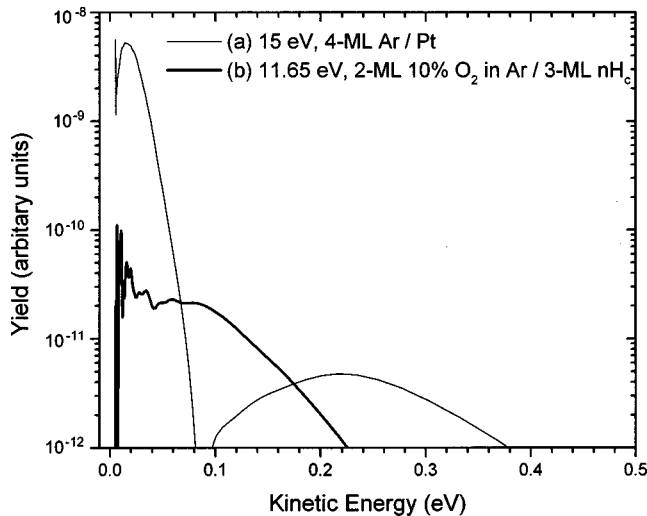


FIG. 4. Kinetic energy distributions of desorbing  $\text{Ar}^*$  atoms. (a) From a 4-ML film of pure Ar deposited on Pt [from the TOF spectrum of Fig. 4(a)]—light line. (b) From a 2-ML  $\text{Ar}/\text{O}_2$  mixture containing 10%  $\text{O}_2$  [from the TOF spectrum of Fig. 4(a)]—heavy line. To obtain these distributions a uniform background was subtracted from the TOF spectra, which were smoothed in Fourier space with a Gaussian filter. The standard transformation correcting channel widths in the time and energy domains was also performed.

component (at 150  $\mu\text{s}$ ) rather than by the fastest (at 100  $\mu\text{s}$ ), which is dominant along the surface normal.<sup>7</sup> The KE distribution of desorbed  $\text{Ar}^*$  atoms is shown in Fig. 4(a). To obtain this figure, a uniform background was subtracted from original data of Fig. 3(a) which was first smoothed with a Gaussian filter. The data is corrected for the nonuniform width of channels in the energy domain.<sup>7</sup>

The intensities of structures seen in the TOF spectrum at 15 eV are essentially unchanged when the Ar film is deposited onto a crystalline *n*-hexane surface (curve *b* in Fig. 3). However, TOF spectra obtained by excitation at  $\sim 11.5$  eV of the  $\text{Ar}^-$  state, differ markedly from those recorded at the higher energy. The TOF spectrum at resonance from a 3-ML-thick Ar film deposited directly onto the Pt in Fig. 3(c) shows both the photon and slow metastable signals seen at the higher energy, together with indications of another metastable component centered at  $\sim 80$   $\mu\text{s}$ . The fast component seen at  $\sim 50$   $\mu\text{s}$  in TOF spectra recorded at 15 eV is absent at the lower energy since excitation of excitons of  $n > 2$  is required to form the antibonding excimer states responsible for this signal.<sup>2,7</sup> The addition of 10%  $\text{O}_2$  enhances considerably the signal peaked at 80  $\mu\text{s}$  and reduces the photon and slow contributions to the NP yield [Fig. 3(d)]. The KE distribution of these desorbing  $\text{Ar}^*$  atoms is illustrated in Fig. 4(b) and is seen to differ significantly from that recorded at 15 eV for pure Ar on the Pt surface; the distribution peaks near 90 meV and extends to several 100 meV. Increasing the concentration of  $\text{O}_2$  from 10% to 50% [Fig. 4(e)] does not significantly affect the TOF spectrum. We believe it likely that the small 80- $\mu\text{s}$  component seen in the pure Ar film, is perhaps due to  $\text{O}_2$  contamination.

## DISCUSSION

### Neutral particle production at energies $>12$ eV

It is clear from the data presented in the previous section that the addition of  $\text{O}_2$  to an argon matrix has several effects

on the desorption processes operating within the mixed  $\text{Ar}/\text{O}_2$  films, notably near an incident energy of 11.5 eV. We first discuss the rapid decrease in NP yield at all energies, at a rate faster than that of Ar replacement by  $\text{O}_2$  in the matrix (i.e., as shown in Fig. 2). This result is consistent with previous experiments that have investigated the effect of  $\text{O}_2$  on the luminescence of Ar films under the impact by 200-eV electrons<sup>25</sup> and MeV light ions.<sup>26</sup> In these latter studies,  $\text{O}_2$  was found to be particularly effective in inhibiting exciton diffusion and reducing the desorbed yield of high KE ( $>200$  meV) Ar (mostly ground state) atoms produced via the formation of the Ar excimer.<sup>25</sup> These effects were attributed to the ionization of  $\text{O}_2$  by free excitons and possibly to the formation of transient ionic clusters.<sup>25</sup> The dissociation of  $\text{O}_2$  via excitation of the Schumann-Runge continuum may also contribute to the reduction of the Ar excimer mean free path although this was not considered to play a dominant role.<sup>25</sup> (Nevertheless,  $^5\text{S O}$ , formed via the dissociation of  $\text{O}_2$  by energy transfer from highly excited Ar atoms with internal excitation energies above 14.3 eV has been observed in gas phase experiments under keV electron bombardment).<sup>27</sup> For comparison, the desorption of Ar atoms of low KE ( $<200$  meV) which was attributed to the CE mechanism, was increased at low  $\text{O}_2$  concentrations, presumably by enhancing exciton trapping close to the film surface.<sup>25</sup> It is instructive to note that desorption via CE is primarily associated with excitation and trapping of the  $n=1$  and  $1'$  surface and bulk excitons.

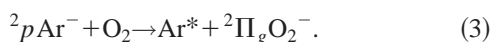
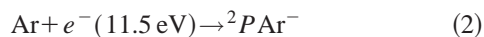
The contrasting behaviors for the low and high KE sputtered atom yields observed in Ref. 25, suggest that the higher energy excitons are more strongly perturbed by the presence of  $\text{O}_2$  in the Ar matrix. The reason for this is easy to identify as  $n > 2$  excitons are of larger physical extent than the lower energy states and are suppressed by decreasing film thickness<sup>28</sup> or cluster size.<sup>29</sup> The radius of the electronic cloud associated with  $n=1$  and  $1'$  excitons is much smaller than the nearest-neighbor distance in Ar,<sup>29</sup> so that these states are less subject to the perturbing effect of  $\text{O}_2$ . Hence we attribute the decrease in NP yields with increasing  $\text{O}_2$  content of the Ar film as essentially due to inhibition of exciton creation and diffusion by  $\text{O}_2$ , especially for excitons of  $n > 2$ .

### Neutral particle production at energies $<12$ eV

The TOF spectra Figs. 3(c)–3(e) indicate that near resonance, desorbed metastable particles rather than photons dominate the NP signal from both pure Ar and  $\text{Ar}/\text{O}_2$  mixture films. This signal can be attributed to  $\text{Ar}^*$  desorption in part because no metastable  $\text{O}_2$  species of an internal energy sufficient to register with our microchannel plate detector has been reported in the literature. Moreover, while metastable O atoms can be created by electron impact excitation of  $\text{O}_2$ , these atomic species have either too small an internal energy to be detected [i.e.,  $\text{O}(^1\text{S})$  and  $\text{O}(^1\text{D})$ ],<sup>30</sup> or have their production thresholds at higher electron energies [i.e.,  $\text{O}(^5\text{S})$  at  $\sim 14.3$  eV].<sup>31</sup> Finally, it should be recalled that our measurements show that in this energy range no metastable particles desorb from pure  $\text{O}_2$  films.

Since in all cases, the peak at  $\sim 11.5$  eV in the NP yield can be associated with metastable Ar desorption, we propose

by analogy with our previous experiments on pure Ar films<sup>16</sup> that the absolute enhancement in desorption reported in Figs. 1(c) and 1(d) is due to reactions of the form



In Eq. (2), the  ${}^2P\text{Ar}^-$  is formed by temporary electron attachment. Subsequently, in Eq. (3), the excess electron is transferred to the oxygen molecule to form a stable  $\text{O}_2^-$  in the  ${}^2\Pi_g$  state and an Ar excited species which eventually desorbs as an Ar\* metastable. Here the oxygen plays the role previously taken by a substrate<sup>16</sup> of suitably large negative  $V_0^S$ , by allowing the electron to be transferred to a subvacuum vibrational level of the  ${}^2\Pi_g$  state. The electron affinity of  $\text{O}_2$  in the  $\nu=0$  level of the  ${}^2\Pi_g$  is  $\sim 0.45$  eV,<sup>32</sup> which is greater than the minimum energy required for Eq. (3) to proceed as calculated from Eq. (1). In practice, the available energy is even larger than 0.45 eV and possibly as great as 1.2 eV once the effect of charge/image charge polarization on the  ${}^2\Pi_g$  is included.<sup>33</sup> The absence of a resonant component to Ar\* desorption from  $\text{N}_2$  doped films is thus attributed to the absence of a subvacuum level  $N_2^-$  state.

It is possible that a reaction similar to the neutralization process discussed above was observed in electron attachment to  $\text{ArO}_4$  clusters, specifically, the formation  $\text{ArO}_4^-$  at an incident electron energy of 11.5 eV as reported by Foltin, Grill, and Märk.<sup>34</sup> In their analysis, the 11.5-eV feature was attributed to the scavenging of a near-zero energy electron by  $\text{O}_2$  following excitation of the lowest Ar excited state. Unfortunately, this interpretation cannot explain the absence of cluster anions following excitation of higher-lying Ar states. Also observed at 11.5 eV,<sup>34</sup> was the production of  $\text{ArO}_3^-$  which was credited to the transfer of charge and energy from an  $\text{Ar}^-$  species to a dissociative state of  $\text{O}_2^-$ . Similar reactions had been observed in thin-film experiments.<sup>10,11</sup> In light of our present results, we reinterpret the  $\text{ArO}_4^-$  signal as being due, at least in part, to a reaction similar to Eq. (3) restricting that the dissociation (desorption) of Ar from the cluster does not proceed.

Despite the involvement of the  ${}^2P\text{Ar}^-$  state in Ar\* desorption from both  $\text{O}_2$ -doped and pure Ar films deposited onto Pt, the ejection mechanisms are different as evidenced by their contrasting TOF spectra. In particular, the increase in the number of metastable atoms having high KE as reported in Fig. 4, is difficult to account for from purely metastable excitation dynamics. We present here a scheme involving the  ${}^2P\text{Ar}^-$  state that provides an explanation for the observation. It shares features with the model proposed by Gadzuk,<sup>35</sup> that was later developed to explain a resonance-like enhancement in the removal of O atoms from an O covered Pd (111) surface under electron bombardment.<sup>36,37</sup> These models in turn share common features with the ‘‘Antoniewicz’’ scheme that described desorption (or dissociation) via excitation of an intermediate cation.<sup>38</sup> It was proposed for the O/Pd system<sup>36,37</sup> that desorption is initiated by electron attachment to a chemisorbed O atom and the formation of a temporary anionic state. The anion, under the influence of charge/image-charge attraction, accelerates towards the Pd surface. After a time interval  $\tau_R$ , the negative ion

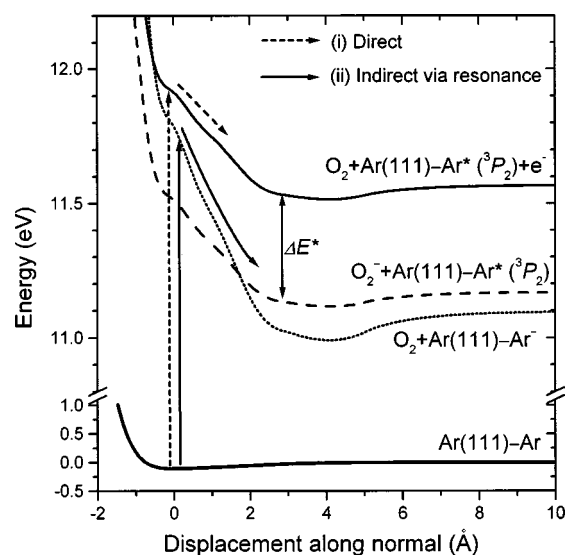


FIG. 5. Calculated potential energy diagram illustrating Ar\* desorption via (i) direct excitation of an Ar\* atom at the film/vacuum interface and (ii) excitation of the  $\text{Ar}^-$  intermediate. Refer to discussion for details.

resonance lifetime, the electron detaches and an O atom is formed close to the metal, on the steeply repulsive inner wall of its chemisorption potential curve such that the repulsion between the O atom and the metal is sufficient to allow desorption.

Figure 5 illustrates the newly proposed desorption model. The lowest potential energy curve in the figure represents the interaction of a ground-state Ar atom with the Ar (111) surface. The horizontal axis represents the displacement from the equilibrium position of the atom along surface normal. The curve is based on the ground-state  $\text{Ar}_2$  potential calculated by Aziz and Chen<sup>39</sup> integrated over a surface atom's nine nearest neighbors (all assumed to be Ar). The uppermost potential energy curve depicts the repulsive interaction of the Ar(111) surface with an  $\text{Ar } {}^3P_2$  metastable atom. The curve is based on that of the  $2u$  state of  $\text{Ar}_2$  as calculated by Castex *et al.*,<sup>40</sup> integrated over the nine nearest Ar neighbors and adjusted such that the dissociation limit corresponds to the excitation energy of the  ${}^3P_2$  state in vacuum. While approximate in nature, the two curves predict an excitation energy of 11.9 eV in the Franck-Condon region, in reasonable agreement with those of Ar surface excitons.<sup>41</sup> Also shown in the figure is a dotted line which we suggest represents the interaction of an  $\text{Ar}^-$  with the Ar film and supporting Pt. Since an excited Ar atom is repelled by the argon's matrix's negative electron affinity, it is likely that an even stronger short-range repulsion exists between the film's surface and the  $\text{Ar}^-$ . This short-range force is undoubtedly opposed by the anion's ability to polarize its environment. Nevertheless, the dissociation limit for a desorbing anion is set by the energies of the gas phase resonances [i.e., 11.1 and 11.27 eV (Ref. 42)] which are considerably lower than those of the condensed phase  ${}^2P$ . For this reason it is reasonable to assume that a net repulsive force exists between the  $\text{Ar}^-$  and the Ar film. Since the excited Rydberg electron cloud density surrounding the Ar anion is twice that of an  $\text{Ar}^*$ , we have represented the surface- $\text{Ar}^-$  potential by multiplying the

surface-Ar\* potential by a factor 2 and translating the curve such that the dissociation limit corresponds to the lower of the two gas-phase resonances.

As illustrated in the figure, Ar atom desorption can be achieved either (i) directly by promoting the atom into the excited neutral state (CE) or (ii) indirectly via the anion state. It is proposed that once formed, the anion moves away from the Ar surface, gaining KE which it largely retains when it is neutralized by electron transfer to a surface O<sub>2</sub> molecule and crosses over onto the dashed curve representing repulsive interaction of the Ar\* with the surface when the electron remains held on the O<sub>2</sub>. This latter curve is simply the same (uppermost) potential energy curve as for a metastable's interaction with the film but translated by an amount  $\Delta E^*$  corresponding to the energy difference between this curve and that for Ar<sup>-</sup> at the displacement where neutralization occurs.

Reference to Fig. 5 indicates that via the direct mechanism, approximately 300 meV of potential energy, is available for desorption of a <sup>3</sup>P<sub>2</sub> atom. However, the measured KE of metastables desorbed via CE, are in the range 20–50 meV,<sup>7</sup> thus considerable energy is transferred to vibrational excitation of the Ar matrix during the desorption process.<sup>7,8</sup> The increase in Ar\* KE at the resonance energy to ~90 meV, seen in Fig. 4, suggests that for the indirect mechanism, the potential energy in the system be at least doubled and requires (in Fig. 5) that the anion move at least ~1.8 Å away from the film before neutralization. If electron transfer occurs with a surface O<sub>2</sub> (assumed to occupy a nearest-neighbor site relative to the Ar<sup>-</sup> in its original position) then the transfer process must be able to occur at distances of up to 4.2 Å. Since electron transfer across larger distances between metastable He atoms and a low work function surface and involving the formation of an He<sup>-</sup> state, have previously been reported<sup>43,44</sup> it seems likely that this latter distance is not too great for transfer to occur. Stressing the approximate nature of the potentials used in Fig. 5, and assuming that the motion of an Ar<sup>-</sup> is determined by its potential energy curve itself approximated by a straight line of slope  $k$  (in eV Å<sup>-1</sup>), elementary considerations imply that

$$\tau = \sqrt{\Delta z \mu / k}, \quad (4)$$

where  $\tau$  represents the time required to move through a distance  $\Delta z$ , and  $\mu$  is the anion's reduced mass. From Eq. (4) we find that roughly  $1.4 \times 10^{-13}$  s is required for the anion to move 1.8 Å. This period is approximately 2.5 times larger than the lifetime of the electron-exciton complex in the bulk [ $\tau_R = 5.6 \times 10^{-14}$  s (Ref. 13)]. When one considers that the resonance lifetime in vacuum<sup>42</sup> (and also probably at the film surface) is greater than  $\tau_R$  and that the increased slope of the anion's potential will lead to faster desorption dynamics and to less vibrational excitation of the matrix, the proposed indirect mechanism appears plausible.

We also note that if, contrary to our previous comments, a *net attractive* potential exists between the Ar<sup>-</sup> anion and the Ar covered Pt substrate, then an enhancement in the KE of desorbed metastables may also occur. This latter would result if an anion accelerated towards the metal, were neutral-

ized by an O<sub>2</sub> such that a metastable atom were formed at a displacement at higher potential energy on the steeply repulsive inner wall of the surface-Ar\* potential. Since some fraction of the KE gained by the Ar<sup>-</sup> as it travels towards the metal would be retained by the metastable atom, a comparatively modest displacement of the anion could substantially alter the KE of a desorbing Ar\*. It is likely that a definitive description of the resonant desorption process will require KE and angular measurements of desorbed ground-state Ar atoms.

While it is envisioned that the indirect desorption mechanism can occur only at the film/vacuum interface, anion formation and neutralization may occur at any point within the film when a <sup>2</sup>PAr<sup>-</sup> is close to an O<sub>2</sub> molecule. Consequently, the metastable yield could contain a low KE component due to exciton trapping and CE following resonantly enhanced exciton formation within the film. This situation can be contrasted to the case of resonant desorption in pure Ar films, where electron transfer can occur only at the film/substrate interface. Thus, in Fig. 1, the Ar<sup>-</sup> state appears at slightly higher energy for the O<sub>2</sub> containing films than for the pure Ar film (i.e. at 11.6 eV rather than 11.4 eV); the decreased polarization energy far from the metal allows the resonance to occur at higher incident energy. A similar effect is likely responsible for the changes in resonance width and energy seen in Fig. 2. At low and intermediate O<sub>2</sub> concentrations, [Figs. 2(b) and 2(c)], one observes a broadening of the resonant feature as resonant processes occurring at the metal, at the film/vacuum interface, and at intermediate points contribute to the desorbed yield. As the O<sub>2</sub> concentration increases the exciton mean free path decreases. Thus at higher O<sub>2</sub> concentrations, [Fig. 2(d)], it is difficult for excitons formed by electron transfer from the resonance into the metal to contribute to the desorbed metastable yield. Instead, the largest proportion of the resonant metastable signal comes from the interaction of Ar<sup>-</sup> with O<sub>2</sub> molecules close to the film/vacuum interface, hence the resonant feature appears narrower and at higher incident energy (i.e., 11.7 eV). For the same reason, the TOF data recorded at the resonance energy for Ar/Pt exhibit essentially only a low KE peak due to CE. In contrast, for 10–50 % by volume O<sub>2</sub> in Ar, only a high KE peak is observed due to the additional energy imparted by electron transfer from Ar<sup>-</sup> to O<sub>2</sub> near the film surface.

## CONCLUSION

We have demonstrated that, in general, the addition of molecular oxygen to thin Ar films inhibits the ESD of metastable atoms, but enhances Ar\* desorption at the energy of the Ar<sup>-</sup> resonance. We have attributed this experimental observation to the ability of O<sub>2</sub> to accept the excess electron of the Ar<sup>-</sup> into a vacant subvacuum level, forming a <sup>2</sup>Π<sub>g</sub> O<sub>2</sub><sup>-</sup> and providing sufficient energy to create a neutral excited Ar\*. In effect this mechanism allows metastable atom desorption to occur at incident electron energies below the minimum energy normally required to electronically excite the film, i.e., the energy of the  $n = 1$  surface exciton.

Time-of-flight measurements show that the Ar\* atoms desorbed following electron transfer between an Ar<sup>-</sup> and an O<sub>2</sub>

are of higher average KE than those desorbed by the cavity expulsion mechanism. We have suggested that is because the desorption dynamics are determined initially by the argon anion's interaction with the Ar film's surface, which we believe to be more steeply repulsive than that of an Ar\*. However, there is a clear need for accurate calculations of the interaction potential between an Ar anion and an Ar film deposited onto a metal substrate. Experimental measurement

of the KE and angular distribution of desorbed ground-state atoms would also be of value.

#### ACKNOWLEDGMENTS

This work was funded by the Medical Research Council of Canada. We wish to thank M. Michaud for his comments regarding this work.

- <sup>1</sup>N. Schwenter, E.-E. Koch, and J. Jortner, *Electronic Excitations in Condensed Rare Gases* (Springer-Verlag, Berlin, 1985).
- <sup>2</sup>G. Zimmerer, Nucl. Instrum. Methods Phys. Res. B **91**, 601 (1994).
- <sup>3</sup>D. E. Weibel, T. Nagai, T. Hirayama, I. Arakawa, and M. Sakurai, Langmuir **12**, 193 (1996).
- <sup>4</sup>G. Zimmerer, J. Low Temp. Phys. **111**, 629 (1998).
- <sup>5</sup>I. Ya. Fugol and E. I. Tarasova, Low Temp. Phys. **23**, 578 (1997).
- <sup>6</sup>G. Leclerc, A. D. Bass, M. Michaud, and L. Sanche, J. Electron Spectrosc. Relat. Phenom. **52**, 725 (1990).
- <sup>7</sup>G. Leclerc, A. D. Bass, A. Mann, and L. Sanche, Phys. Rev. B **46**, 4865 (1992).
- <sup>8</sup>Shengting Cui, R. E. Johnson, and P. T. Cummings, Phys. Rev. B **39**, 9580 (1989).
- <sup>9</sup>M. Sakurai, T. Hirayama, and I. Arakawa, Vacuum **41**, 217 (1990).
- <sup>10</sup>P. Rowntree, L. Parenteau, and L. Sanche, Chem. Phys. Lett. **182**, 479 (1991).
- <sup>11</sup>P. Rowntree, H. Sambe, L. Parenteau, and L. Sanche, Phys. Rev. B **47**, 4537 (1993).
- <sup>12</sup>M. Michaud, P. Cloutier, and L. Sanche, Phys. Rev. B **47**, 4131 (1993).
- <sup>13</sup>M. Michaud, P. Cloutier, and L. Sanche, Phys. Rev. B **48**, 11 336 (1993).
- <sup>14</sup>G. J. Schulz, Rev. Mod. Phys. **45**, 378 (1973).
- <sup>15</sup>J. N. H. Brunt, G. C. King, and F. H. Read, J. Phys. B **10**, 1289 (1977).
- <sup>16</sup>A. D. Bass, E. Vichnevetski, P. Cloutier, and L. Sanche, Phys. Rev. B **57**, 14 914 (1998); **60**, 5078 (1999).
- <sup>17</sup>G. Perluzzo, G. Bader, L. G. Caron, and L. Sanche, Phys. Rev. Lett. **55**, 545 (1985).
- <sup>18</sup>M. Michaud and L. Sanche, J. Electron Spectrosc. Relat. Phenom. **51**, 237 (1990).
- <sup>19</sup>E. Vichnevetski, P. Cloutier, and L. Sanche, J. Chem. Phys. **110**, 8112 (1999); E. Vichnevetski and L. Sanche, Langmuir **15**, 6851 (1999).
- <sup>20</sup>L. Sanche, J. Chem. Phys. **71**, 4860 (1979).
- <sup>21</sup>M. A. Strzhemechny, A. I. Prokhvatilov, and L. D. Yantsevich, Physica B **198**, 267 (1994).
- <sup>22</sup>S. J. Buckman and C. W. Clark, Rev. Mod. Phys. **66**, 539 (1994).
- <sup>23</sup>L. G. Caron, G. Perluzzo, G. Bader, and L. Sanche, Phys. Rev. B **33**, 3027 (1986).
- <sup>24</sup>H. Shi, P. Cloutier, and L. Sanche, Phys. Rev. B **52**, 5385 (1995).
- <sup>25</sup>E. Hudel, E. Steinacker, and P. Feulner, Phys. Rev. B **44**, 8972 (1991).
- <sup>26</sup>C. T. Reimann, W. L. Brown, and R. E. Johnson, Phys. Rev. B **37**, 1455 (1998).
- <sup>27</sup>T. Mori, K. Kanou, Yo-ichi Ishikawa, and S. Arai, J. Chem. Phys. **96**, 8258 (1992).
- <sup>28</sup>P. Feulner, T. Müller, A. Puschnann, and D. Menzel, Phys. Rev. Lett. **59**, 791 (1987).
- <sup>29</sup>J. Wörmer, R. Karnbach, M. Joppien, and T. Möller, J. Chem. Phys. **104**, 8269 (1996).
- <sup>30</sup>E. C. Zipf in *Electron-Molecule Interactions and Their Applications*, edited by L. G. Christophorou (Academic, Orlando, 1984), Vol. 1, Chap. 4.
- <sup>31</sup>W. L. Borst and E. C. Zipf, Rev. A **4**, 153 (1971).
- <sup>32</sup>A. A. Christodoulides, D. L. McCorkle, and L. G. Christophorou, in *Electron-Molecule Interactions and Their Applications*, edited by L. G. Christophorou (Academic, Orlando, 1984), Vol. 2, Chap. 4, Table 2.
- <sup>33</sup>L. Sanche and M. Deschênes, Phys. Rev. Lett. **61**, 2096 (1988).
- <sup>34</sup>M. Foltin, V. Grill, and T. D. Märk, Chem. Phys. Lett. **188**, 427 (1992).
- <sup>35</sup>J. W. Gadzuk, Phys. Rev. B **31**, 6789 (1985).
- <sup>36</sup>A. Hoffman, Xingcai Guo, J. T. Yates, Jr., J. W. Gadzuk, and C. W. Clark, J. Chem. Phys. **90**, 5793 (1989).
- <sup>37</sup>J. W. Gadzuk and C. W. Clark, J. Chem. Phys. **91**, 3174 (1989).
- <sup>38</sup>P. R. Antoniewicz, Phys. Rev. B **21**, 3811 (1980).
- <sup>39</sup>R. A. Aziz and H. H. Chen, J. Chem. Phys. **67**, 5719 (1977).
- <sup>40</sup>M. C. Castex, M. Morlais, F. Spiegelmann, and J. P. Malrieu, J. Chem. Phys. **75**, 5006 (1981).
- <sup>41</sup>M. Michaud and L. Sanche, Phys. Rev. B **50**, 4725 (1994).
- <sup>42</sup>P. Hammond, J. Phys. B **29**, L231 (1996).
- <sup>43</sup>J. Lee, C. Hanrahan, J. Arias, F. Bozso, R. M. Martin, and H. Metiu, Phys. Rev. Lett. **54**, 1440 (1985).
- <sup>44</sup>A. G. Borisov, D. Teillet-Billy, and J. P. Gauyacq, Surf. Sci. **284**, 337 (1993); **325**, 323 (1994).